Orbital-free molecular dynamics simulations of melting in Na_8 and Na_{20}: Melting in steps

Andrés Aguado,[a] José M. López, and Julio A. Alonso
Departamento de Física Teórica, Universidad de Valladolid, Valladolid 47011, Spain

Malcolm J. Stott
Department of Physics, Queen's University, Kingston, Ontario K7L 3N6, Canada

(Received 31 July 1998; accepted 12 July 1999)

The melting-like transitions of Na_8 and Na_{20} are investigated by *ab initio* constant energy molecular dynamics simulations using a variant of the Car–Parrinello method which employs an explicit electronic kinetic energy functional of the density, thus avoiding the use of one-particle orbitals. Several melting indicators are evaluated in order to determine the nature of the various transitions, and are compared with other simulations. Both Na_8 and Na_{20} melt over a wide temperature range. For Na_8, a transition is observed to begin at ~110 K, between a rigid phase and a phase involving isomerizations among the different permutational isomers of the ground state structure. The ''liquid'' phase is completely established at ~220 K. For Na_{20}, two transitions are observed: the first, at ~110 K, is associated with isomerization transitions among those permutational isomers of the ground state structure which are obtained by interchanging the positions of the surface-like atoms; the second, at ~160 K, involves a structural transition from the ground state isomer to a new set of isomers with the surface molten. The cluster is completely liquid at ~220 K. © *1999 American Institute of Physics.* [S0021-9606(99)01937-6]

I. INTRODUCTION

Recent experimental advances have made possible the study of the melting phenomenon in metal clusters. Martin[1] measured the melting temperatures T_m of large sodium clusters by observing the disappearance of the atomic shell structure with increasing temperature, and determined the dependence of T_m on cluster size. More recently, Haberland and co-workers[2] determined the heat capacity and melting temperature of free sodium clusters containing from 50 to 200 atoms by studying the temperature dependence of the photofragmentation mass spectrum. In addition, electron diffraction patterns of trapped clusters[3] may be useful for distinguishing different stages in the melting process.

For many years, computer simulations have been the main guide to an understanding of melting-like transitions in small finite systems. Molecular dynamics (MD) calculations based on phenomenological potentials have been used to study the solid-like to liquid-like phase transitions in rare gas,[4] alkali halide,[5,6] and metal[7–14] clusters. The unification of density functional theory (DFT) and molecular dynamics formulated by Car and Parrinello[15] allows explicit treatment of the electronic degrees of freedom. Such *ab initio* molecular dynamics calculations have been performed by Röthlisberger and Andreoni[16] for Na_n $(n=2-20)$ microclusters at several temperatures, and very recently, Rytkönen *et al.*[17] have presented results for the melting of Na_{40}. These studies make use of the Kohn–Sham (KS) version of DFT,[18] but large computational savings can be obtained if an orbital-free method, based solely in the electronic density $n(\mathbf{r})$, is used instead. Madden and co-workers[19] have demonstrated the value of orbital-free methods for the study of bulk metallic systems. Shah *et al.*[20] and Govind *et al.*[21] have applied the approach to study the structures of small metal and covalent clusters. Blaise *et al.*[22] have performed orbital-free calculations of some static and dynamic properties of sodium clusters with sizes up to 274 atoms, and Vichare and Kanhere[23] have studied the melting of Al_{13}. In this article we describe the study of solid-like to liquid-like phase transitions of Na_8 and Na_{20} microclusters using constant energy orbital free molecular dynamics simulations.

In Sec. II we present theoretical details of the method. The results are presented and discussed in Sec. III. In Sec. IV is a summary of the main conclusions from this study.

II. THEORY

A. Car–Parrinello molecular dynamics with orbital-free energy density functionals

The orbital-free molecular dynamics method is a Car–Parrinello total energy scheme which uses an explicit kinetic-energy functional of the electron density, and has the valence electron density as the dynamic variable. Now we describe the main features of the energy functional. The orbital-free calculational scheme has been described at length in Refs. 19–22, so we will give just a brief description here.

The ground state energy is a functional of the valence electron density $n(\mathbf{r})$, and a function of the ion positions $\mathbf{R}_n$ $(n=1,2,...,N)$, with the following form (Hartree atomic units will be used throughout this article):

[a]Electronic mail: aguado@jmlopez.fam.cie.uva.es

$$E[n,\mathbf{R}]=T_s(n)+\frac{1}{2}\int\int\frac{n(\mathbf{r})n(\mathbf{r}')}{|\mathbf{r}-\mathbf{r}'|}d\mathbf{r}d\mathbf{r}'+\int n(\mathbf{r})V_{\text{ext}}(\mathbf{r})d\mathbf{r}+E_{XC}[n]+E_{\text{ion-ion}}[\mathbf{R}], \quad (1)$$

where the different terms are the kinetic energy functional for a noninteracting inhomogeneous electron gas, the classical electron–electron interaction energy, the interaction energy between the valence electrons and the external potential provided by the instantaneous ionic configuration, the exchange-correlation energy functional, and the classical Coulomb repulsion between positive ions. Three key approximations in the energy functional involve $T_s[n]$, $E_{XC}[n]$, and the electron–ion interaction. The electronic kinetic energy functional used in this work corresponds to the gradient expansion around the homogeneous limit through second order,[24]

$$T_s[n]=T^{\text{TF}}[n]+\lambda T^W[n], \quad (2)$$

where the first term is the Thomas–Fermi approximation,

$$T^{\text{TF}}[n]=\frac{3}{10}(3\pi^2)^{2/3}\int_\Omega n(\mathbf{r})^{5/3}d\mathbf{r}, \quad (3)$$

and T^W (the Weizsäcker term) is the lowest-order gradient correction to T^{TF},

$$T^W[n]=\frac{1}{8}\int_\Omega\frac{|\nabla n(\mathbf{r})|^2}{n(\mathbf{r})}d\mathbf{r}, \quad (4)$$

taking some account of inhomogeneities in the electron density. Different values have been proposed in the literature for the constant λ. The value adopted here, $\lambda=\frac{1}{9}$, corresponds to the limit of a slowly varying $n(\mathbf{r})$ and has a number of desirable properties.[25–27] The local density approximation (LDA) is used for the exchange-correlation functional. We use the Perdew and Zunger parametrization[28] of the electron gas results of Ceperley and Alder.[29] The external field contains the electron–ion interaction, $V_{\text{ext}}(\mathbf{r})=\Sigma_i v(\mathbf{r}-\mathbf{R}_i)$, where we take for v the local pseudopotential of Fiolhais *et al.*,[30] which reproduces very well the properties of bulk sodium and has shown good transferability to sodium clusters.[31] Although some progress has been made recently for including the effects of nonlocality in the pseudopotential in orbital-free schemes,[32] these effects are expected to be small for sodium. The ion–ion interactions are treated using the usual Ewald method.[33]

For a given set of ion positions $\{\mathbf{R}\}$, that is for a given external potential V_{ext}, the ground state is obtained from the variational principle

$$\frac{\delta}{\delta n(\mathbf{r})}\left(E[n,\mathbf{R}]-\mu\int n(\mathbf{r})d\mathbf{r}\right)=0, \quad (5)$$

where μ is the electron chemical potential chosen to give the desired number of electrons N_e. We have found it convenient to work in terms of a single effective orbital $\psi(\mathbf{r})$ rather than $n(\mathbf{r})$, where

$$n(\mathbf{r})=|\psi(\mathbf{r})|^2, \quad (6)$$

TABLE I. Bond length and binding energy per atom for Na_2 and Na_6, calculated by Perdew and co-workers (Ref. 31) using the Kohn–Sham all-electron (KSAE) and Kohn–Sham pseudopotential (KSPS) methods compared to our results of the gradient expansion functional of Eq. (2) with the same pseudopotential (GEPS).

	Bond length (a.u.)		Binding energy (eV)	
	Na_2	Na_6	Na_2	Na_6
KSAE	5.64	6.51	0.44	0.63
KSPS	5.77	6.87	0.46	0.53
GEPS	5.99	6.81	0.55	0.69

and to vary ψ rather than n. This has the advantage of maintaining n nonnegative if ψ is real. The cluster of interest is placed in a unit cell of a superlattice of volume Ω, and the set of plane waves periodic in the superlattice is used to expand ψ. The expansion coefficients $C_{\mathbf{G}}$ (where $\mathbf{G}$ is a reciprocal lattice vector of the superlattice) are considered as generalized coordinates of a set of fictitious classical particles each of mass m.[15] The Lagrangian for the whole system of electrons and ions is

$$L(C,\dot{C},\mathbf{R})=\sum_{\mathbf{G}}\frac{1}{2}m|\dot{C}_{\mathbf{G}}|^2+\sum_{i=1}^{N}\frac{1}{2}M_i\dot{\mathbf{R}}_i^2-E[n,\mathbf{R}], \quad (7)$$

and the constraint to be considered is

$$\int_\Omega d\mathbf{r}n(\mathbf{r})=\Omega\sum_{\mathbf{G}}C_{\mathbf{G}}^*C_{\mathbf{G}}=N_e, \quad (8)$$

where N_e is the number of electrons per supercell, and M_i is the mass of the ith ion.

The explicit functional of the density we have used for the electronic energy is far superior in computational speed and memory requirements to the conventional KS orbital approach, allowing the treatment of larger systems for longer simulation times. Those computational savings can also be used to perform simulations for a larger number of different temperatures, allowing better identification of transition temperatures. Since the present restriction to local pseudopotentials is not a serious matter for sodium, the most important difference between the orbital-free and KS approaches is the treatment of the independent particle kinetic energy. $T_s[n]$ is computed exactly in the KS approach, whereas the orbital-free approach draws on approximate density functionals based on a few known limiting cases. Our choice for $T_s[n]$ with $\lambda=\frac{1}{9}$ is appropriate for a slowly varying density, whereas $T_s[n]=T^W[n]$ is believed to give the limit of rapidly varying density. Linear response theory gives $T_s[n]$ when the variations in electron density about the mean density are small, and some functionals attempt to combine these different limits.[19] Our functional would seem to be appropriate for the smooth pseudoelectron density of a Na cluster, but since little is known about the range of validity of the various functionals, we have performed test calculations on some simple Na systems and compared the results with those of other approaches.

Table I presents results for equilibrium bond lengths and binding energies per atom for the Na dimer and an octahedral Na_6 cluster calculated with three different approximations. All the calculations use the LDA for exchange and correlation, but differ in their treatment of the electron–ion

interaction and the electron kinetic energy. The results[31] of KS all-electron calculations are given along with those of KS calculations which use our choice of local pseudopotential, and comparison of these results tests the pseudopotential of Fiolhais *et al.*[30] We see that the use of the pseudopotential overestimates the bond lengths by 2%–3%, but the increased bond length in Na_6 over that in the dimer is reproduced. The binding energies, with respect to spin-polarized free atoms, are also in reasonable agreement. The third set of calculations uses the same pseudopotential and the orbital-free kinetic energy functional. A comparison of the second and third sets of results tests the orbital-free $T_s[n]$. The approximate $T_s[n]$ overestimates the bond length of the dimer by 4% but the results for Na_6 are in very good agreement. The binding energies (with respect to spin-polarized free atoms) are overestimated but the increased binding in Na_6 is reproduced. The agreement between orbital-free and KS calculations for the ground state structure and energetic ordering of the low lying isomers of Na_8, which is detailed in Sec. III, and the reasonably accurate interatomic distances we obtain provide additional support to our approach for studying the melting-like transitions of Na clusters. This agreement suggests that the orbital-free approach gives a potential energy surface with the correct features for interatomic separations near the equilibrium distances, and this is enough to determine details of the melting transition. The discrepancies in the binding energies are less important for the dynamics provided we do not consider evaporation events.

The main approximation of an orbital-free method is neglect of quantum shell effects. Specifically, the method gives energies that vary smoothly as a function of cluster size, without showing the oscillations associated with electronic shell closures. On the other hand, ionic shell effects due to the geometrical arrangement of ions are present. The experimental results of Haberland *et al.*[2] seem to indicate that both effects are relevant to the melting of sodium clusters, although their relative importance is not yet known. Nevertheless, the good performance of the orbital-free method mentioned above, together with the good agreement between the melting dynamics of Na_8 and Na_{20} predicted by our model and that obtained from the KS calculations of Röthlisberger and Andreoni[16] (see Sec. III), support the orbital-free method as a valuable starting point. Extended Thomas–Fermi models usually give equilibrium structures that are quite spherical and that do not have the deformations found in small clusters of size intermediate between two electronic shell closures. By restricting our study to closed-shell clusters, which are known to be quite spherical, we minimize the probability of finding wrong zero-temperature isomers.

The calculations for Na_8 and Na_{20} have been performed using a cubic supercell of edge 63.58 a.u. with a $64\times64\times64$ mesh and a plane wave energy cutoff for ψ of 10 Rys. The test calculations performed for Na_2 and Na_6 showed that with this cutoff equilibrium bond lengths converge within 0.01 Å and binding energies within 0.002 eV, which we consider sufficient for our purposes. The equations of motion were integrated using the Verlet algorithm[34] for both the electrons and the ions with a time step ranging from $\Delta t = 1\times10^{-15}$ s for the simulations performed at the lowest temperatures to $\Delta t = 0.85\times10^{-15}$ s for those performed at the highest ones. The fictitious electron mass ranged from 1.15×10^8 a.u. for the shorter time steps to 1.75×10^8 a.u. for the longest. These choices resulted in a better than 0.1% conservation of total energy. The first step in the simulation was the determination of the low temperature ground state (GS) structures of Na_8 and Na_{20} (using the dynamical simulated annealing technique[15]) by heating the clusters to 600 K and then slowly cooling them. Next, several molecular dynamics simulation runs at different energies were performed in order to obtain the caloric curve. The initial relative positions of the atoms in the cluster for the first run were taken by deforming the equilibrium geometry slightly. The final configuration for each run served as the starting geometry for the next run at a different energy. The initial velocities for every new run were obtained by scaling the final velocities of the preceding run. The total simulation times were 8 ps for the lowest temperatures for which the clusters are very rigid ($T < 60$ K) and 20–22 ps for temperatures larger than 60 K. Longer runs of 50–60 ps were performed for specific temperatures. The first 2 ps of each run were not included in the various time averages. After velocity scaling was performed at the beginning of each new trajectory, the internal cluster temperature (see Sec. II B) was always an oscillating function of time with a decreasing envelope during approximately the first 2 ps of the simulation, after which equilibration is achieved. The reason for such a short equilibration time seems to be that the velocity scaling never increased the cluster temperature by more than 20 K, at least not in the transition region. The equilibration was also checked by comparing the caloric curve and the specific heat curve (see Sec. II B). The locations of the specific heat peaks were coincident with the slope changes in the caloric curve, which is a sign of correct equilibration.

B. Analysis of the molecular dynamics

In order to characterize the thermal behavior of the clusters as a function of increasing internal energy, as well as the solid-like to liquid-like transitions, we monitor (a) global quantities that are calculated from time averages over a whole trajectory at a given energy and (b) time dependent quantities that are calculated from averages over well separated time origins along a single trajectory.

First, we define the ''internal temperature'' T of the cluster as[4,35]

$$T = \frac{2}{(3N-6)k_B}\langle E_{\mathrm{kin}}\rangle_t, \tag{9}$$

where k_B is the Boltzmann constant, E_{kin} is the ionic kinetic energy, and $\langle\ \rangle_t$ represents the time average over a whole trajectory. All the global quantities described below will be plotted as functions of this internal temperature.

The degree of mobility of the atoms—a sort of index of the rigidity of the cluster—can be characterized by the relative root-mean-square (rms) bond length fluctuation δ, defined by[4,35]

$$\delta = \frac{2}{N(N-1)} \sum_{i>j} \frac{(\langle R_{ij}^2 \rangle_t - \langle R_{ij} \rangle_t^2)^{1/2}}{\langle R_{ij} \rangle_t}, \tag{10}$$

where $R_{ij} = |\mathbf{R}_i - \mathbf{R}_j|$. This quantity changes abruptly at isomerization or melting transitions and, for the bulk, a sharp increase in δ gives the Lindemann criterion for melting.

As another indicator of the melting-like transition we calculate the specific heat defined by[4,35]

$$C = \left[N - N\left(1 - \frac{2}{3N-6}\right) \langle E_{\mathrm{kin}} \rangle_t \langle E_{\mathrm{kin}}^{-1} \rangle_t \right]^{-1}. \tag{11}$$

This magnitude is related to the fluctuations in the ionic kinetic energy, and has peaks (corresponding to slope changes in the caloric curve) associated with some phase transitions.

The mean square displacement, $R(t)$, is defined by

$$R(t) = \frac{1}{N n_t} \sum_{j=1}^{n_t} \sum_{i=1}^{N} [\mathbf{r}_i(t_{0_j} + t) - \mathbf{r}_i(t_{0_j})]^2, \tag{12}$$

where n_t is the number of time origins (t_{0_j}) considered along a trajectory, and is a time-dependent quantity that also serves as a measure of the rigidity of the cluster.[4] The slope of $R(t)$ for large t is proportional to the diffusion coefficient. Thus, a flat $R(t)$ curve is indicative of a solid-like cluster with the constituent atoms vibrating about their equilibrium positions; when diffusive motion of the atoms starts, the slope of $R(t)$ becomes positive. We shall see in Sec. III that it is useful to separate the atoms of Na_{20} into two subsets of $N_c = 2$ ''core'' and $N_s = 18$ ''surface'' atoms. We can then define partial $R(t)$'s, restricted to core $[R_c(t)]$ and surface $[R_s(t)]$ atoms, respectively, and the differences between these will be indicators of different degrees of rigidity in the two groups of atoms for a given internal cluster temperature.

Recently,[36] ''atomic equivalence indexes,''

$$\sigma_i(t) = \sum_j |\mathbf{r}_i(t) - \mathbf{r}_j(t)|, \tag{13}$$

which contain very detailed structural information, have been introduced. The degeneracies in $\sigma_i(t)$ are due to the specific symmetry of the isomer under consideration, and the variations in the time evolution of $\sigma_i(t)$ allow detailed examination of the melting mechanism.

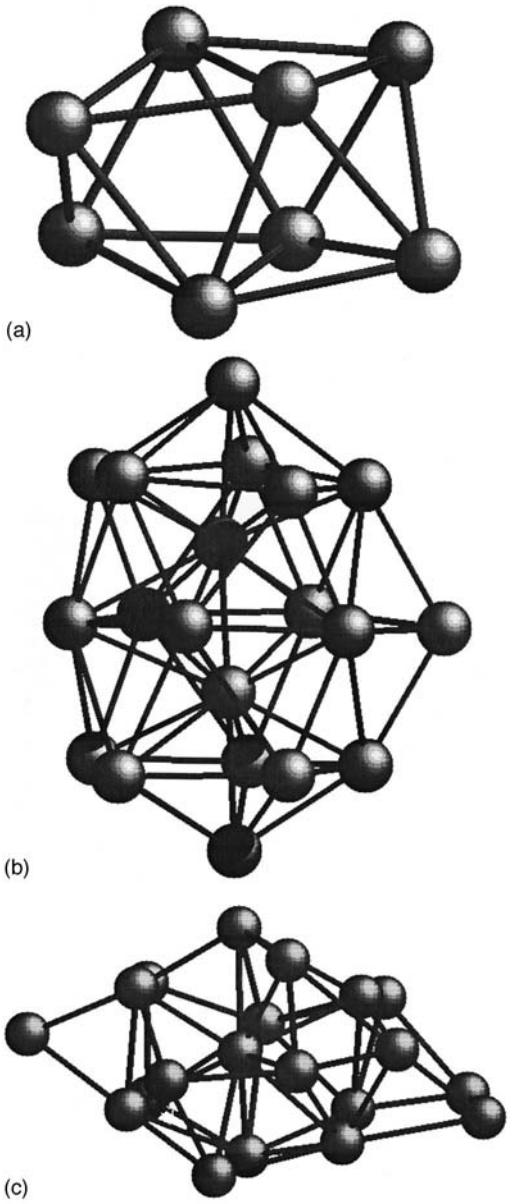

FIG. 1. Geometries of the ground state isomers of (a) Na_8 and (b) Na_{20}. (c) An example of the (19+1) structure that appears after the second phase transition in Na_{20} (see the text for details).

III. RESULTS AND DISCUSSION

A. Na_8

The calculated GS structure of Na_8 is shown in Fig. 1(a). It is a dodecahedron (D_{2d} symmetry), a result which is in agreement with the KS-LDA calculations.[16,37,38] The stellated tetrahedron (T_d symmetry) is the GS structure in all-electron self-consistent field-configuration interaction SCF-CI calculations,[39,40] although the energy difference between the isomers is very small indeed. It is of note that the orbital-free LDA calculations lead to the same energetic ordering of isomers (and also to similar energy differences between isomers) as the KS-LDA.

Figure 2 shows the results for the calculated global quantities C [Fig. 2(a)] and δ [Fig. 2(b)] as functions of internal cluster temperature, and the time evolution of the mean square displacement, $R(t)$, for three representative temperatures [Fig. 2(c)]. The specific heat shows a peak centered at a temperature $T_{m_1} \approx 110$ K, which correlates with the temperature region in which δ experiences an almost stepwise increase, and which marks the onset of the melting transition. This is followed by a steady increase of $\delta(T)$, until a leveling off occurs at $T_{m_2} \approx 220$ K, indicating that the liquid state is fully developed. The melting transition of Na_8 from a rigid form in which the atoms merely oscillate about the equilibrium configuration to a ''fluid'' form characterized by uncorrelated motion of the atoms is spread over a range of temperatures $T = T_{m_1} - T_{m_2}$. Figure 2(c) shows that, for a temperature $T = 34$ K, $R(t)$ has zero slope at long times, reflecting the oscillatory motion of the atoms. At $T = 111$ K the diffusive motion of the atoms in the cluster begins, resulting in a positive slope which increases with temperature.

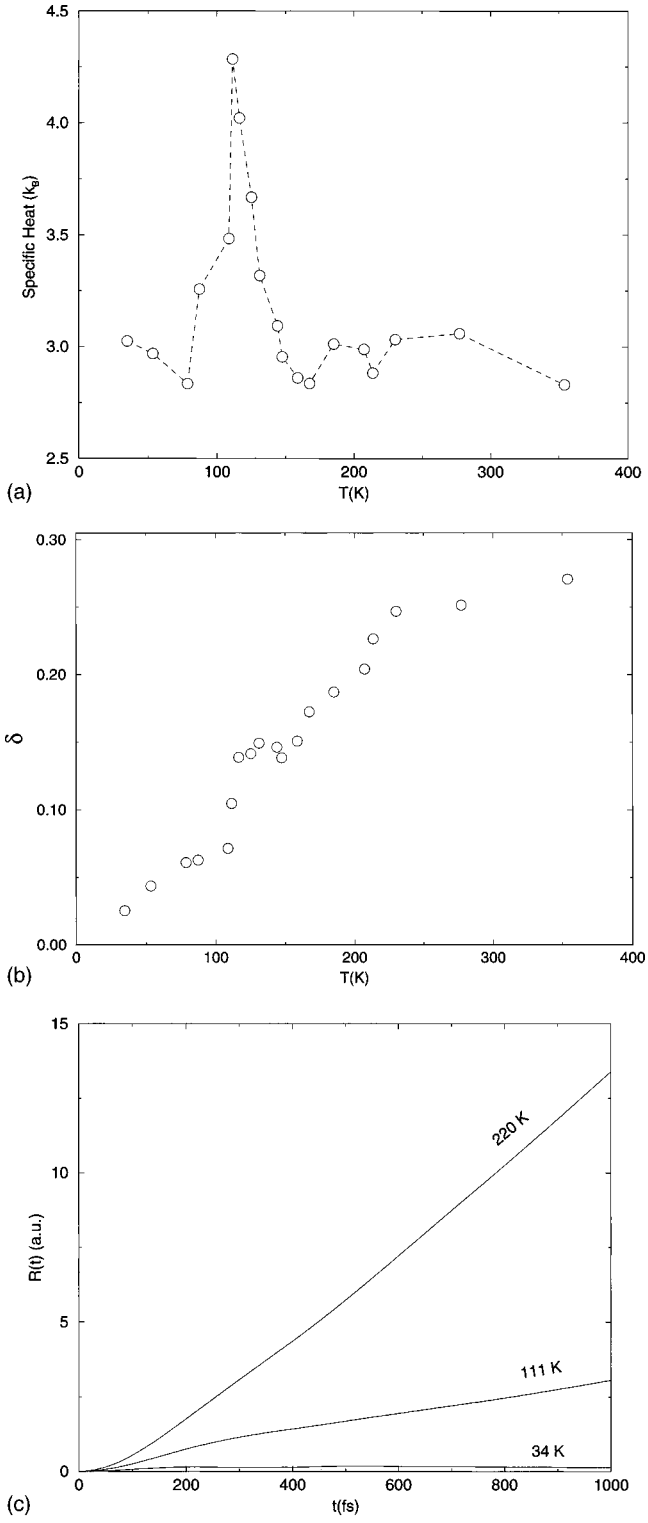

FIG. 2. (a) Specific heat and (b) relative rms bond length fluctuation of Na_8 as functions of the internal temperature. The deviation around the mean temperature is smaller than the size of the circles. (c) Mean square displacement as a function of time for three representative values of T.

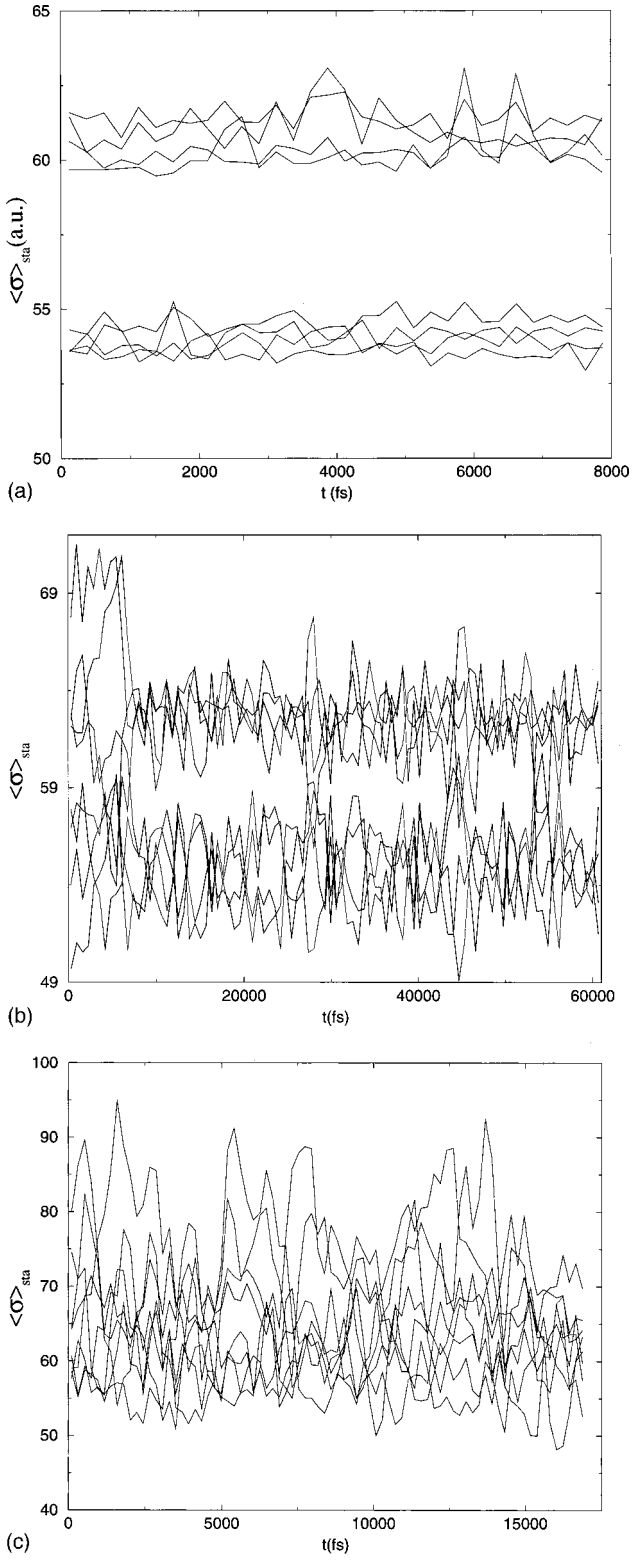

FIG. 3. Short-time averaged atomic equivalence indexes as functions of time for Na_8 at T=(a) 34, (b) 111, and (c) 220 K. Note the different simulation times for different temperatures.

The quantities shown in Fig. 2 indicate that Na_8 undergoes a melting-like transition in the temperature range 110–220 K. In order to get a better understanding of the melting, the short-time averages (sta) of the atomic equivalence indexes, $\langle\sigma_i(t)\rangle_{sta}$, have been calculated and the cluster evolution during the trajectories has been followed visually using computer graphics. The $\langle\sigma_i(t)\rangle_{sta}$ curves are presented in Fig. 3 for three representative values of T. At the lowest temperature $T=34$ K [Fig. 3(a)] there are two distinct groups of nearly equivalent atoms in the D_{2d} GS structure: four atoms with coordination 4, and four with coordination 5. The

curve crossings within a group of nearly equivalent atoms display oscillations of the atoms around their equilibrium positions, but there is no crossing of the curves from different groups. At a higher temperature $T=78\,\mathrm{K}$ (not shown), but still lower than T_{m_1}, the oscillations have larger amplitudes, but the two types of atoms do not yet mix. At $T=111\,\mathrm{K}$, which marks the beginning of the step in δ, interchanges between atoms with different coordination begin, but are still scarce. The dynamics over 60 ps [Fig. 3(b)] illustrates that the atoms in the cluster can still be separated into two sets with 4 and 5 coordination during most of the simulation time, since there are just four interchange events. The moving pictures of these oscillators show that the onset of melting in Na_8 is associated with isomerization transitions among the different permutational isomers of the D_{2d} GS structure, which come with significant distortions of the cluster from the GS geometry. The transitions become more frequent and the distortions increasingly severe with increasing temperature, giving rise to the steady increase observed in δ, until at $T\approx 220\,\mathrm{K}$ [Fig. 3(c)] and higher temperatures the ground state isomer is seen only occasionally in the movies. Snapshots of the trajectories at these temperatures show that the cluster sometimes adopts elongated configurations with Na or Na_2 subunits joined to the cluster by a single bond. This is reflected in Fig. 3(c) by the larger values of $\langle\sigma_i\rangle_{\mathrm{sta}}$. All the atoms diffuse across the cluster volume so that the different $\langle\sigma_i\rangle_{\mathrm{sta}}$ curves are all mixed and the ''liquid'' phase is fully established. While we have not observed evaporation of fragments at this temperature (at least within 20 ps), the trajectories suggest that Na or Na_2 subunits may evaporate at higher temperatures from the ends of a ''cigar-like'' cluster. However, our energy functional may not be reliable for such events.

Detailed simulations of the melting-like transition of Na_8 have been performed by Bulgac and co-workers[7] using constant-temperature MD simulations with a phenomenological interatomic potential and by Poteau, Spiegelmann and Labastie (PSL)[10] using Monte Carlo (MC) simulations with a tight-binding Hamiltonian to describe the electronic system; recently, Calvo and Spiegelmann[14] (CS) have also performed MC simulations employing an empirical potential. Aside from the differences between the MC and MD methods, the main difference between those calculations and our work is the interatomic potential. That employed by Bulgac has free parameters fitted to properties of bulk sodium and, while the tight-binding calculations of PSL deal explicitly with the electronic system, some overlap integrals were fitted to *ab initio* results for the sodium dimer and tetramer. Since we consider the electronic degrees of freedom explicitly and find the forces on ions through the Hellman–Feynman theorem, the present calculations should be considered an advance over empirical or semiempirical methods. Bulgac predicts a transition temperature of about 100 K from a solid-like to a glassy phase of the cluster in which the atoms stay close to their equilibrium positions for relatively long periods with occasional atom interchanges. The tight binding treatment[10] gives a melting-like transition at ~200 K, whereas CS give an approximate value of 80–100 K for T_m, more similar to our values and those of Bulgac. Bulgac also predicts a boiling transition at 900 K but we do not expect our approach to be reliable at such high temperatures where evaporation is a factor. However, the ''solid-to-glassy'' transition is similar to the behavior we have found at the onset of melting at ~110–130 K, where the atoms remain in their equilibrium positions for relatively long periods, only swapping positions from time to time with a frequency that increases with temperature. For temperatures above 220 K where the value of δ increases smoothly with T, we find that the atoms are very mobile and that the cluster can be considered liquid.

Röthlisberger and Andreoni (RA)[16] have performed finite temperature simulations for Na_8 using the *ab initio* Car–Parrinello MD method with pseudopotentials for the electron–ion interaction and the LDA for the exchange-correlation energy functional. Thus, the main difference from the present calculations is our use of an approximate electronic kinetic-energy functional. They deduced from a simulation at $T=240\,\mathrm{K}$ a value of δ that is still less than the 0.1 value which is taken to indicate the onset of melting according to the Lindeman criterion. The full KS method gives a more accurate description of the electronic structure than our orbital-free approach, but we feel that the apparently contradictory results for δ can be reconciled. The total simulation time of RA for Na_8 was $t=6$ ps, corresponding to about ~10 vibrational periods for sodium.[1] Our calculated value of δ at $T=230\,\mathrm{K}$, if we average over the first 6 ps of the simulation is 0.098, in agreement with the full KS results. Due to the nature of the melting transition in Na_8, which involves repeated swapping of the atom positions, 6 ps may not be long enough to obtain a converged value for δ. In fact, we chose the total simulation time of $t=20$ ps after recognizing that preliminary simulations performed with $t=8$ ps did not yield a converged result for δ. With $t=20$ ps, further increases only lead to minor changes in δ, at least when the cluster is clearly liquid like. Nevertheless, we cannot guarantee that fully converged values of δ have been obtained in the transition region.

B. Na_{20}

We find the ground state structure of Na_{20} to be a single-capped double icosahedron [Fig. 1(b)], again in good agreement with the KS-LDA calculations of RA,[16] who found this structure to be almost degenerate with their GS structure. The variation of the specific heat with temperature, which is shown in Fig. 4(a), displays two maxima around 110 and 170 K. The relative rms bond length fluctuation is given in Fig. 4(b). For small temperatures the curve $\delta(T)$ has a small positive slope, reflecting the thermal expansion of the solid-like cluster, but at higher temperatures there are two abrupt increases at $T_{m_1}\approx 110\,\mathrm{K}$ and $T_{m_2}\approx 160\,\mathrm{K}$, and a leveling off at $T_{m_3}\approx 220\,\mathrm{K}$, indicating that the melting of Na_{20} occurs in several stages over the range of temperatures $T_{m_1}-T_{m_3}$. The two peaks in the specific heat are in rough correspondence with the two steps in $\delta(T)$, but the leveling off in δ does not seem to be associated with any pronounced feature in the specific heat. The mean square displacement for the particles in the cluster is plotted as a function of time in Fig. 4(c) for

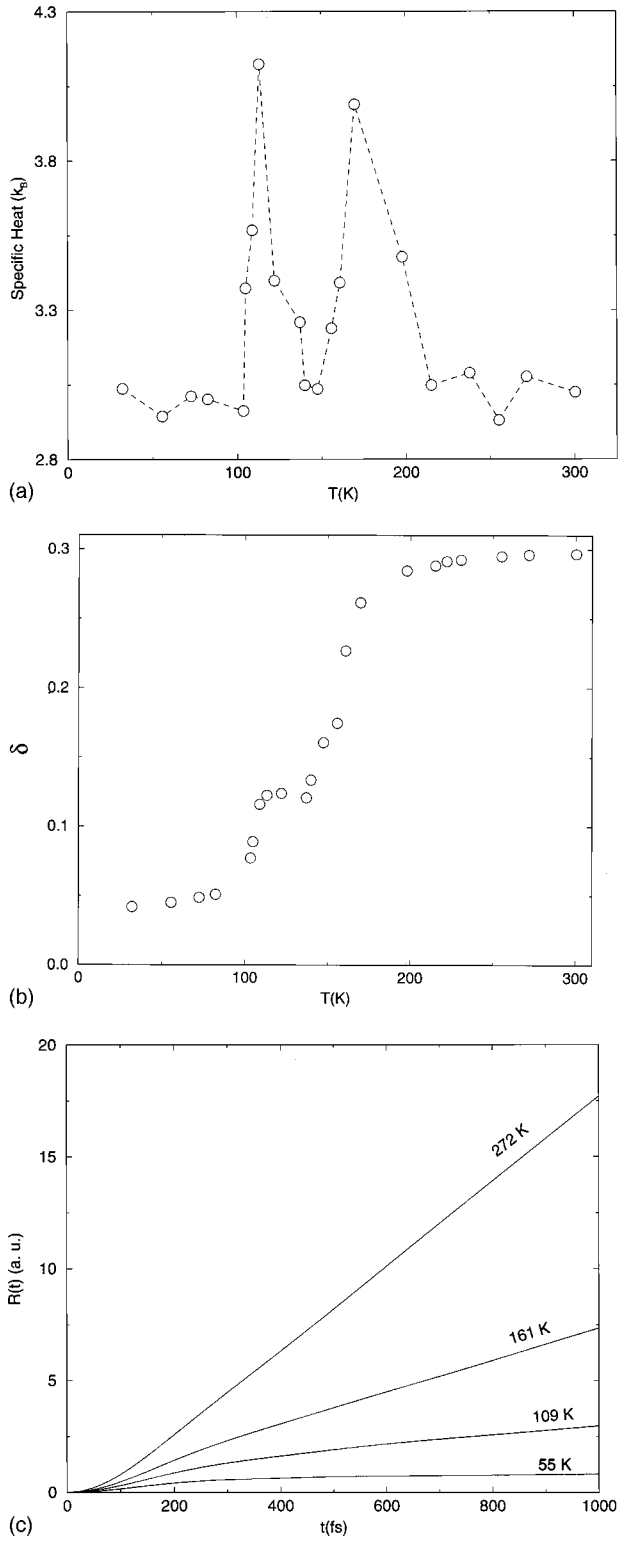

FIG. 4. (a) Specific heat and (b) relative rms bond length fluctuation of Na_{20} as functions of the internal temperature. The deviation around the mean temperature is smaller than the size of the circles. (c) Mean square displacement as a function of time for four representative values of T.

four different temperatures. The curve corresponding to $T=55\,\mathrm{K}$ shows a clear leveling off after a small initial rise, reflecting the solid-like nature of the cluster at that temperature. For $T=109\,\mathrm{K}$ and higher temperatures, $R(t)$ shows a linear increase, implying a finite diffusion coefficient and the emergence of liquid-like properties.

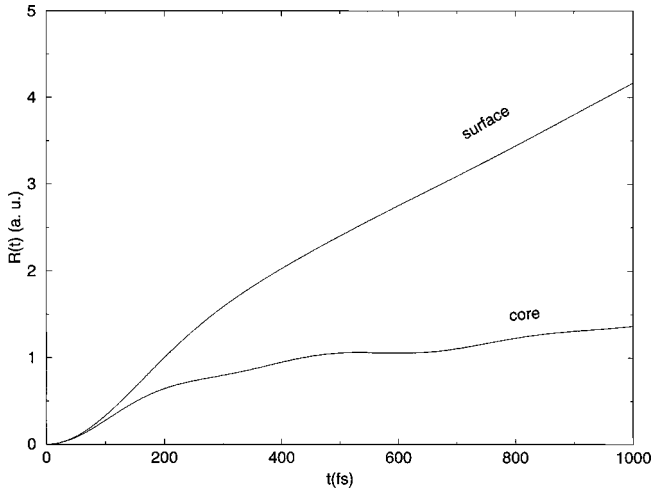

FIG. 5. Partial mean square displacements for core $[R_c(t)]$ and surface $[R_s(t)]$ atoms in Na_{20} for $T=109\,\mathrm{K}$.

In order to investigate the nature of the transitions we divide the 20 atoms of the cluster into two subsets: the two internal ''core'' atoms of the ground state structure, and the 18 peripheral ''surface'' atoms. The partial $R_c(t)$ and $R_s(t)$ for the temperature at which the first step in δ begins are shown in Fig. 5. The $R_s(t)$ curve shows the typical diffusive behavior of liquid-like phases, whereas $R_c(t)$, after the initial rise, oscillates with an average slope near zero. Differences in the mobility of the surface and core atoms are clearly indicated, with the surface atoms undergoing diffusive motion at a temperature ($T_{m_1}\approx 110\,\mathrm{K}$) lower than that necessary for the diffusion of the core atoms. Snapshots at regular time intervals for the runs between $T=T_{m_1}$ and T_{m_2} show the two central atoms oscillating around their initial positions, while surface atoms interchange their positions in the cluster without destroying the double-icosahedral symmetry. The picture is similar to the onset of melting in Na_8. The swapping of surface atom positions causes significant distortions of the double-icosahedron geometry, but after each interchange the cluster returns to the ground state structure. Therefore, we identify the transition at $T_{m_1}\approx 110\,\mathrm{K}$ as an isomerization-like transition in which the cluster begins to visit those permutational isomers of the ground state which involve the interchange of positions between surface atoms. In our view, this fluctuating phase of Na_{20} cannot be associated with surface melting, because the double-icosahedral symmetry persists and the surface disorder is temporary.

The next stage is seen in snapshots from the runs performed at temperatures between T_{m_2} and T_{m_3}. The second transition involves the motion of one of the central atoms out to a peripheral position, the double-icosahedral symmetry is lost, and most of the snapshots show a structure with a single central atom [see an example of this in Fig. 1(c)]. The central core atom exchanges with one of the 19 surface atoms at a slower rate than the interchanges between surface atoms, and so converged values of δ require longer simulations (50–60 ps). The 19 surface atoms are very mobile and the structure

of the cluster fluctuates a great deal. The exploration of a new structure at these temperatures leads to the second peak in the specific heat, and we identify $T_{m_2} \approx 160\,\mathrm{K}$ with an isomerization-like transition in which new (19+1) structures are explored. As the temperature is increased from T_{m_2} to T_{m_3}, the interchanges of a core atom and a surface atom become more frequent, leading to the steady increase in δ and a cluster surface which has melted in the sense that the structure is now very fluid and the surface disorder is large.

In Fig. 6 we show the short-time averaged $\sigma_i(t)$ for several representative temperatures. At $T=32\,\mathrm{K}$ [Fig. 6(a)] the cluster is solid like and $\langle \sigma_i(t) \rangle_{\mathrm{sta}}$ serves to identify groups of ''nearly'' equivalent atoms. Starting from the bottom, they are the 2 central atoms, the 5 atoms of the central pentagon, the 10 atoms in the upper and lower pentagons, and finally the 2 axial atoms and the capping atom. At $T=72\,\mathrm{K}$ (not shown) the different groups can still be recognized, but Fig. 6(b) shows that at 137 K there is a group of two central atoms, but the rest are no longer distinguishable. At $T=163\,\mathrm{K}$ [Fig. 6(c)] we see that the cluster has a single central atom for most of the simulation time (56 ps), the 19 atom surface is melted, and occasionally an interchange between the central atom and one of the surface atoms occurs. At higher temperatures the interchange rate increases.

Simulations of the melting-like transitions of Na_{20} have also been performed by Bulgac,[7] PSL,[10] and CS.[14] As for Na_8, the ground state structure of Na_{20} predicted by PSL is different from that of KS-LDA calculations, although it may also be divided into core and surface atoms. They also predict surface melting at a temperature of $T_s=190\,\mathrm{K}$ and a melting temperature of $T_m=300\,\mathrm{K}$. The discrepancies between these quantities and the corresponding quantities we obtain should again be attributed to the differences in the interatomic interactions. Once more our detailed description of the onset of the melting transition and the full establishment of a liquid-like phase are in better agreement with the results of Ju and Bulgac.[7] CS predict the same ground state structure found in this work for Na_{20}. Their calculations also predict a two-step melting mechanism, with $T_{m_1} \approx 100\,\mathrm{K}$ and $T_{m_2} \approx 200\,\mathrm{K}$.[14] RA[16] have performed two short *ab initio* KS-LDA molecular dynamics simulations of Na_{20}. At $T=350\,\mathrm{K}$, the lowest temperature they considered, they found that the mobility of the atoms in Na_{20} is already quite high within the 3 ps of their simulation, but such a short simulation time led to a value of $\delta \approx 0.1$. If we average over the first 3 ps of our run performed at $T=324\,\mathrm{K}$, we obtain $\delta=0.15$, in contrast with the converged value $\delta=0.29$. A simulation time of 3 ps, corresponding to ~ 5 vibrational periods, does not allow enough jumps to obtain a converged value of δ.

The melting-like transitions in both Na_8 and Na_{20} are found to be spread over a broad temperature range, and in the case of Na_{20} we have identified a stepwise melting mechanism. Recently, Rey *et al.*[41] in a study of the melting-like transition of a 13 particle cluster associated the occurrence of melting in steps to the softness of the repulsive core interaction rather than to any many-body character of the interactions. For the softer potentials considered, two abrupt increases of δ were found: the first corresponding to the onset of isomerization transitions involving only surface atoms, and the second to complete melting. The stepwise melting mechanism was less clearly defined for the harder interatomic potentials. We have used our approximate functional in a series of static calculations for Na_2 at several interatomic distances in order to construct the binding energy curve, and

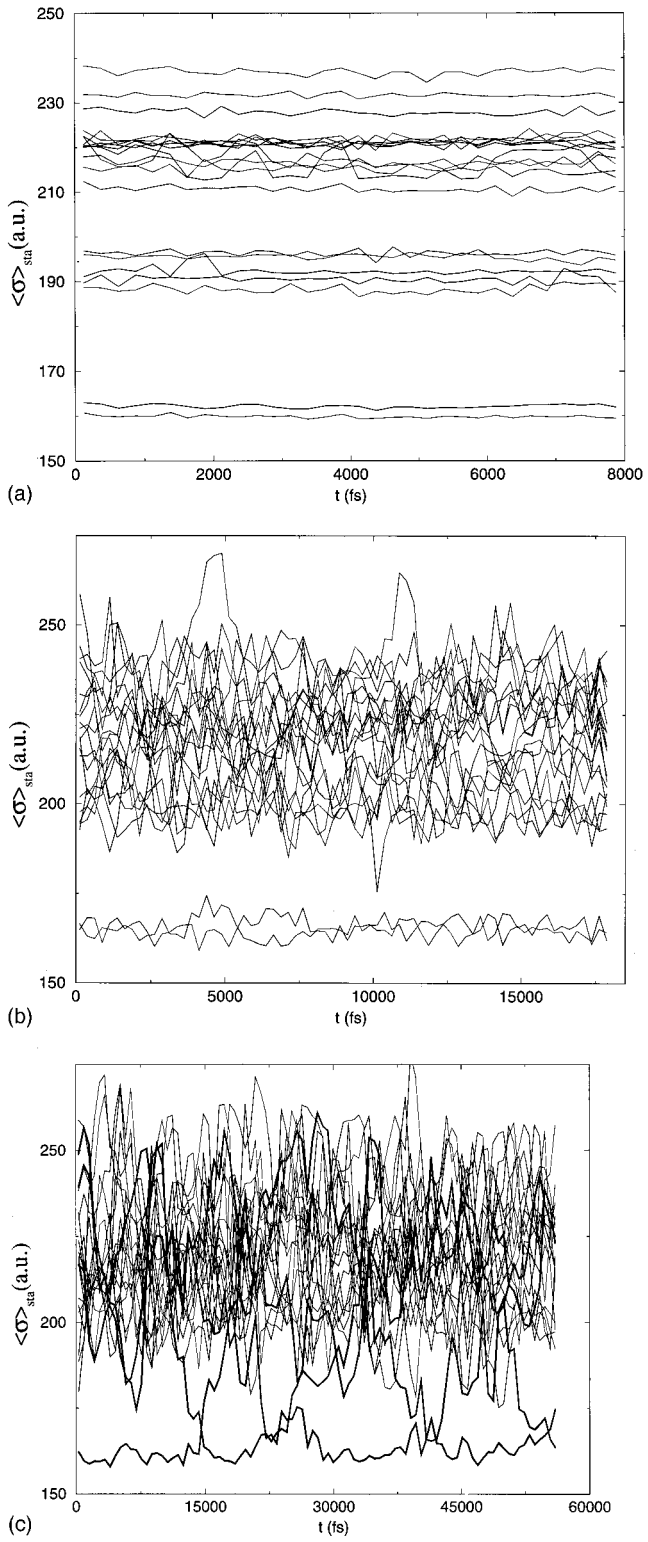

FIG. 6. Short-time averaged atomic equivalence indexes as functions of time for Na_{20} at T=(a) 32, (b) 137, and (c) 156 K. Note the different simulation times for each temperature.

have compared it to the interatomic potentials considered by Rey *et al.*[41] We find that the repulsive part of the binding energy curve obtained using the GEPS is softer than their softest interatomic potential, so the stepwise melting we have found is consistent with their findings.

Jellinek *et al.*[42] have demonstrated for Li_8 that the temperature at which exploration of low-lying isomers begins is estimated more accurately in MC than in MD simulations. This is because the *J*-walk MC sampling of the configurational space is not hindered by the presence of energy barriers. If the energy in a microcanonical MD simulation is just slightly higher than the energy needed to surmount a barrier, exceedingly long simulation times will be needed in order to achieve an efficient sampling. Thus, the real temperatures at which the onset of melting occurs may be slightly lower than those determined in our ''short'' simulations. The location of the specific heat peaks, however, should be more accurate, because these occur for a temperature higher than that corresponding to the onset of melting, where the energy is already large enough to easily surmount the barriers. In summary, the *width* of the specific heat peaks may be underestimated in MD simulations.

We have studied the melting of clusters upon heating, but some differences might be observed if the clusters were cooled from a high temperature simulation. Details of the melting transition, such as the number and location of the steps in the δ curve, depend on the specific isomer from which the dynamics is started, and thus may differ from those obtained through a cooling procedure. This is worthy of further study.

IV. SUMMARY

We have applied an *ab initio*, density-based, molecular dynamics method to the study of melting transitions in finite atomic systems. The computational effort that is required is modest in comparison with that required by the traditional CP-MD technique based on the use of KS one-particle orbitals. The computational effort to update the electronic system scales linearly with the system size N, in contrast to the N^3 scaling of orbital-based methods. This saving allows the method to be used in the study of large clusters and also for performing extensive MD simulations in much the same way as the usual procedures involving phenomenological potentials.

The method has been applied here to study the melting-like transitions in Na_8 and Na_{20} clusters. Na_8 melts in a broad temperature range from 110 to 220 K. The transition at $\sim$100 K is from a rigid cluster in which the atoms are vibrating around their fixed equilibrium positions to a phase in which the different permutational isomers of the GS structure are visited. For higher temperatures the cluster distorts more and more from the GS structure and can be considered fully liquid at $T \approx 220$ K. Na_{20} undergoes several successive transformations with increasing temperature, and the melting transition is also spread over a wide temperature range. In the first transition at $T_{m_1} \approx 110$ K surface atoms swap positions without destroying the underlying icosahedral symmetry. At $T_{m_2} \approx 160$ K, one of the inner atoms becomes surface like, the other remains in its central position for most of the simulation time, and the surface of the cluster has melted. Swapping between the central atom and one of the surface atoms is more frequent upon heating, until at $T_{m_3} \approx 220$ K the value of δ saturates. As expected, the temperatures of the melting intervals are lower than the experimental melting temperature of bulk Na ($T_m^{bulk} = 371$ K). Preliminary calculations to simulate the melting of bulk Na give a melting temperature that is in very good agreement with experiment, which gives us confidence in the quantitative results we obtained for the melting temperatures of the clusters.

Our findings suggest that it is important to study several melting indicators when disentangling details of melting-like transitions. If a stepwise mechanism is present, the location of the different steps is clearly indicated in δ. The variation of the diffusion coefficient with temperature obtained from the $R(t)$ curves is also useful in this respect. The atomic equivalence indexes are valuable for understanding the nature of the structural transitions associated with each step in δ. We conclude that the specific heat alone may not be a sensitive indicator of all the ''structural'' information contained in the δ curve. Specifically, the final leveling off in δ, marking the end of the transition region and the temperature at which the liquid-like phase is completely established, does not have any appreciable feature associated with it in the specific heat.

Comparison with other theoretical calculations performed at different levels of theory suggests that our results agree with the *ab initio* KS-LDA calculations of Röthlisberger and Andreoni if the same simulation times are considered. This agreement is a strong validation of our model. However, we found it necessary to lengthen the simulation times to at least 20 ps (and sometimes to 50–60 ps) in order to obtain converged global quantities. With the improved statistics, our results for Na_8 and Na_{20} are in better agreement with those of Bulgac and co-workers and of Calvo and Spiegelmann than with those of Poteau *et al.*

ACKNOWLEDGMENTS

This work has been supported by DGES (Grant No. PB95-0720-C02-01), NATO (Grant No. CRG.961128), and the Junta de Castilla y León (VA63/96 and VA72/96). The authors wish to thank L. E. González, M. J. López, and P. A. Marcos for useful discussions. One of the authors (A.A.) acknowledges a graduate fellowship from the Junta de Castilla y León. A second author (M.J.S.) acknowledges support by the NSERC of Canada.

[1] T. P. Martin, Phys. Rep. **273**, 199 (1996).
[2] M. Schmidt, R. Kusche, W. Kronmüller, B. von Issendorff, and H. Haberland, Phys. Rev. Lett. **79**, 99 (1997); M. Schmidt, R. Kusche, B. von Issendorff, and H. Haberland, Nature (London) **393**, 238 (1998); R. Kusche, T. Hippler, M. Schmidt, B. von Issendorff, and J. Habevland, Eur. Phys. J. D **9**, 1 (1999).
[3] Z. L. Wang, J. M. Petroski, T. C. Green, and M. A. El-Sayed, J. Phys. Chem. B **102**, 6145 (1998); M. Maier-Borst, D. B. Cameron, M. Rokni, and J. H. Parks, Phys. Rev. A **59**, R3162 (1999).
[4] J. Jellinek, T. L. Beck, and R. S. Berry, J. Chem. Phys. **84**, 2783 (1986); H. L. Davis, J. Jellinek, and R. S. Berry, *ibid.* **86**, 6456 (1987); T. L. Beck, J. Jellinek, and R. S. Berry, *ibid.* **87**, 545 (1987).
[5] J. P. Rose and R. S. Berry, J. Chem. Phys. **96**, 517 (1992) **98**, 3246

(1993); **98**, 3262 (1993); V. K. W. Cheng, J. P. Rose, and R. S. Berry, Surf. Rev. Lett. **3**, 347 (1996).
[6] F. Calvo and P. Labastie, J. Phys. Chem. B **102**, 2051 (1998).
[7] A. Bulgac and D. Kusnezov, Phys. Rev. Lett. **68**, 1335 (1992); Phys. Rev. B **45**, 1988 (1992); N. Ju and A. Bulgac, *ibid.* **48**, 2721 (1993).
[8] Z. B. Güvenc and J. Jellinek, Z. Phys. D **26**, 304 (1993).
[9] C. Rey, L. J. Gallego, J. García-Rodeja, J. A. Alonso, and M. P. Iñiguez, Phys. Rev. B **48**, 8253 (1993); J. García-Rodeja, C. Rey, L. J. Gallego, and J. A. Alonso, *ibid.* **49**, 8495 (1994).
[10] R. Poteau, F. Spiegelmann, and P. Labastie, Z. Phys. D **30**, 57 (1994)
[11] M. Fosmire and A. Bulgac, Phys. Rev. B **52**, 17509 (1995); Z. Phys. D **40**, 458 (1997).
[12] A. Bulgac, Z. Phys. D **40**, 454 (1997); J. M. Thompson and A. Bulgac, *ibid.* **40**, 462 (1997).
[13] C. L. Cleveland, W. D. Luedtke, and U. Landman, Phys. Rev. Lett. **81**, 2036 (1998).
[14] F. Calvo and F. Spiegelmann, Phys. Rev. Lett. **82**, 2270 (1999).
[15] R. Car and M. Parrinello, Phys. Rev. Lett. **55**, 2471 (1985).
[16] U. Röthlisberger and W. Andreoni, J. Chem. Phys. **94**, 8129 (1991).
[17] A. Rytkönen, H. Häkkinen, and M. Manninen, Phys. Rev. Lett. **80**, 3940 (1998).
[18] W. Kohn and L. J. Sham, Phys. Rev. **140**, 1133A (1965).
[19] M. Pearson, E. Smargiassi, and P. A. Madden, J. Phys.: Condens. Matter **5**, 3221 (1993); E. Smargiassi and P. A. Madden, Phys. Rev. B **49**, 5220 (1994); M. Foley, E. Smargiassi, and P. A. Madden, J. Phys.: Condens. Matter **6**, 5231 (1994); E. Smargiassi and P. A. Madden, Phys. Rev. B **51**, 117 (1995); **51**, 129 (1995); M. Foley and P. A. Madden, *ibid.* **53**, 10589 (1996); B. J. Jesson, M. Foley, and P. A. Madden, *ibid.* **55**, 4941 (1997); J. A. Anta, B. J. Jesson, and P. A. Madden, *ibid.* **58**, 6124 (1998).
[20] V. Shah, D. Nehete, and D. G. Kanhere, J. Phys.: Condens. Matter **6**, 10773 (1994); D. Nehete, V. Shah, and D. G. Kanhere, Phys. Rev. B **53**, 2126 (1996); V. Shah and D. G. Kanhere, J. Phys.: Condens. Matter **8**, L253 (1996); V. Shah, D. G. Kanhere, C. Majumber, and G. P. Das, *ibid.* **9**, 2165 (1997).
[21] N. Govind, J. L. Mozos, and H. Guo, Phys. Rev. B **51**, 7101 (1995).
[22] P. Blaise, S. A. Blundell, and C. Guet, Phys. Rev. B **55**, 15856 (1997).
[23] A. Vichare and D. G. Kanhere, J. Phys.: Condens. Matter **10**, 3309 (1998).
[24] *Theory of the Inhomogeneous Electron Gas*, edited by S. Lundqvist and N. H. March (Plenum, New York, 1983).
[25] P. Hohenberg and W. Kohn, Phys. Rev. **136**, 864B (1964).
[26] W. Yang, Phys. Rev. A **34**, 4575 (1986).
[27] J. P. Perdew, Phys. Lett. A **165**, 79 (1992).
[28] J. P. Perdew and A. Zunger, Phys. Rev. B **23**, 5048 (1981).
[29] D. Ceperley and B. Alder, Phys. Rev. Lett. **45**, 566 (1980).
[30] C. Fiolhais, J. P. Perdew, S. Q. Armster, J. M. McLaren, and H. Brajczewska, Phys. Rev. B **51**, 14001 (1995); **53**, 13193 (1996).
[31] F. Nogueira, C. Fiolhais, J. He, J. P. Perdew, and A. Rubio, J. Phys.: Condens. Matter **8**, 287 (1996).
[32] S. Watson, B. J. Jesson, E. A. Carter, and P. A. Madden, Europhys. Lett. **41**, 37 (1998).
[33] P. P. Ewald, Ann. Phys. (Leipzig) **64**, 253 (1921).
[34] L. Verlet, Phys. Rev. **159**, 98 (1967); W. C. Swope and H. C. Andersen, J. Chem. Phys. **76**, 637 (1982).
[35] S. Sugano, *Microcluster Physics* (Springer, Berlin, 1991).
[36] V. Bonacić-Koutecký, J. Jellinek, M. Wiechert, and P. Fantucci, J. Chem. Phys. **107**, 6321 (1997); D. Reichardt, V. Bonacić-Koutecký, P. Fantucci, and J. Jellinek, Chem. Phys. Lett. **279**, 129 (1997).
[37] J. L. Martins, J. Buttet, and R. Car, Phys. Rev. B **31**, 1804 (1985).
[38] J. M. Pacheco and W. D. Schöne, Phys. Rev. Lett. **79**, 4986 (1997).
[39] V. Bonacić-Koutecký, P. Fantucci, and J. Koutecký, Phys. Rev. B **37**, 4369 (1988).
[40] F. Spiegelmann and D. Pavolini, J. Chem. Phys. **89**, 4954 (1988).
[41] C. Rey, J. García-Rodeja, L. J. Gallego, and M. J. Grimson, Phys. Rev. E **57**, 4420 (1998).
[42] J. Jellinek, S. Srinivas, and P. Fantucci, Chem. Phys. Lett. **288**, 705 (1998).